DNA binding by the MATα2 transcription factor controls its access to alternative ubiquitin-modification pathways

Christopher M. Hickey, Yang Xie, and Mark Hochstrasser*
Department of Molecular Biophysics & Biochemistry, Yale University, New Haven, CT 06520

ABSTRACT **Like many transcription factors, the yeast protein MATalpha2 (α2) undergoes rapid proteolysis via the ubiquitin-proteasome system (UPS). At least two ubiquitylation pathways regulate α2 degradation: one pathway utilizes the ubiquitin ligase (E3) Doa10 and the other the heterodimeric E3 Slx5/Slx8. Doa10 is a transmembrane protein of the endoplasmic reticulum/inner nuclear membrane, whereas Slx5/Slx8 localizes to the nucleus and binds DNA nonspecifically. While a single protein can often be ubiquitylated by multiple pathways, the reasons for this "division of labor" are not well understood. Here we show that α2 mutants with impaired DNA binding become inaccessible to the Slx5/Slx8 pathway but are still rapidly degraded through efficient shunting to the Doa10 pathway. These results are consistent with the distinct localization of these E3s. We also characterized a novel class of DNA binding-defective α2 variants whose degradation is strongly impaired. Our genetic data suggest that this is due to a gain-of-function interaction that limits their access to Doa10. Together, these results suggest multiple ubiquitin-ligation mechanisms may have evolved to promote rapid destruction of a transcription factor that resides in distinct cellular subcompartments under different conditions. Moreover, gain-of-function mutations, which also occur with oncogenic forms of human transcription factors such as p53, may derail this fail-safe system.**

Monitoring Editor
William P. Tansey
Vanderbilt University

Received: Oct 10, 2017
Revised: Dec 19, 2017
Accepted: Dec 27, 2017

INTRODUCTION

The ubiquitin-proteasome system (UPS) is responsible for most selective protein degradation in eukaryotic cells (Varshavsky, 2012). Ubiquitin is a small protein that can be covalently attached to other proteins in a process known as *ubiquitylation*. Ubiquitylation is catalyzed by a cascade of three enzymes: ubiquitin-activating enzyme (E1), ubiquitin-conjugating enzyme (E2), and ubiquitin ligase (E3). All eukaryotes encode multiple E2s and many E3s, allowing a wide range of proteins to be specifically ubiquitylated under a variety of cellular conditions. E3s typically directly associate with substrate proteins and are the main source of specificity within the UPS.

Ubiquitin modifications occur most commonly on lysine side chains of substrates, though exceptions are known (Wang *et al.*, 2009; Weber *et al.*, 2016). Ubiquitin itself has seven lysine residues, and any of these lysines, as well as its N-terminal amino group, can be modified with additional ubiquitins, giving rise to polyubiquitin chains. While ubiquitylation of a protein can affect the modified protein in many ways, the prototypical fate of polyubiquitylated substrates is degradation by the proteasome (Inobe and Matouschek, 2014).

Among the most common substrates of the UPS are transcription factors (Geng *et al.*, 2012). We have long studied proteolysis of the yeast *Saccharomyces cerevisiae* transcription factor MATα2 (α2), the first endogenous protein demonstrated to be a substrate of the UPS (Hochstrasser and Varshavsky, 1990; Hochstrasser *et al.*, 1991; Hickey, 2016). Yeast exist as one of three cell types: either of two haploid types (a or α), which can mate to generate the third type, and an a/α diploid (Haber, 2012). Yeast cell types are maintained by transcription factors that control genes involved in cell-fate determination. These transcription factors are expressed from

This article was published online ahead of print in MBoC in Press (http://www.molbiolcell.org/cgi/doi/10.1091/mbc.E17-10-0589) on January 3, 2018.

*Address correspondence to: Mark Hochstrasser (mark.hochstrasser@yale.edu).

Abbreviations used: 3HA, triple hemagglutinin and hexahistidine tags; asg, aspecific gene; *Deg*, degradation signal: E3, ubiquitin ligase; EMSA, electrophoretic mobility shift assay; ER, endoplasmic reticulum; MAT, mating type; SD, synthetic defined; STUbL, SUMO-targeted ubiquitin ligase; SUMO, small ubiquitin-like modifier; UPS, ubiquitin-proteasome system.

the mating type (*MAT*) locus, which carries either a-type or α-type information. The *MAT*α locus encodes two proteins: α2, which represses seven specific a-specific genes, and α1, which promotes expression of several α-specific genes. Most wild haploid yeast can rapidly switch mating types in a process that involves replacing the information at the *MAT* locus with a DNA cassette encoding the opposite cell-type information from a silenced locus. While cells of α type that undergo gene conversion to a type at the *MAT* locus will no longer synthesize new α2, phenotypic switching is inhibited unless the existing α2 protein is degraded by the UPS (Laney and Hochstrasser, 2003).

Rapid degradation of α2 involves two distinct ubiquitylation pathways (Figure 1A) (Chen *et al.*, 1993; Swanson *et al.*, 2001; Xie *et al.*, 2010). One utilizes the Doa10 E3 operating with two E2s, Ubc6 and Ubc7; all three proteins are tightly associated with the endoplasmic reticulum (ER)/nuclear envelope (NE) (Swanson *et al.*, 2001). The other pathway is likely to involve more than one E3, but the main E3 is the heterodimeric Slx5/Slx8 working with the E2 Ubc4 (Xie *et al.*, 2010). Slx5/Slx8 is localized to the nucleus, and the Slx8 subunit has been shown to bind DNA in a nonspecific manner (Yang *et al.*, 2006; Cook *et al.*, 2009).

Slx5/Slx8 has affinity for the small ubiquitin-like modifier (SUMO) protein, which can be conjugated to proteins in a process analogous to that for ubiquitin but involving enzymes specific for SUMO. Prior SUMO modification of proteins can stimulate their Slx5/Slx8-mediated ubiquitylation (Uzunova *et al.*, 2007; Xie *et al.*, 2007). E3s from multiple organisms, including humans, have been characterized to have properties similar to Slx5/Slx8, and these E3s are collectively called SUMO-targeted ubiquitin ligases (STUbLs) (Sriramachandran and Dohmen, 2014). However, α2 is not detectably sumoylated in vivo, and its degradation does not require an active sumoylation pathway; moreover, Slx5/Slx8 can ubiquitylate α2 in vitro in the absence of SUMO (Xie *et al.*, 2010). Thus, Slx5/Slx8 can act in a SUMO-independent manner, an activity also observed for the *Drosophila* STUbL Degringolade (Abed *et al.*, 2011).

Direct interaction of α2 with DNA is mediated through its homeodomain (Figure 1B) (Hall and Johnson, 1987). The a-specific gene operators feature two α2 homeodomain-binding sites flanking binding sites for the protein Mcm1, and the two proteins bind cooperatively to this DNA motif (Vershon and Johnson, 1993). Interaction of α2 with Mcm1 is mediated through a mostly hydrophobic interface involving a central linker domain of α2 (Mead *et al.*, 1996).

The hydrophobic motif in the α2 linker also contributes to the Ubc4-dependent pathway of α2 degradation (Hickey and Hochstrasser, 2015). While the α2 linker domain is not sufficient to drive degradation in vivo, a fragment of α2 consisting of the linker and homeodomain is rapidly degraded. This fragment of α2 is referred to as *Deg2* (*Deg*radation signal-*2* or *Deg*ron-*2*). A degron is defined here as a protein fragment that is sufficient for promoting the degradation of proteins containing it (Hickey, 2016). We use the term "degradation element" to describe any region of a proteolytic substrate that is necessary for degron function. The first degron identified in α2 is called *Deg1*, an N-terminal fragment of α2 that is targeted exclusively by the Doa10 pathway (Hochstrasser and Varshavsky, 1990; Swanson *et al.*, 2001). Though both the linker and homeodomain are required for a functional *Deg2* in vivo, Slx5/Slx8 recognizes the homeodomain of α2 and not the linker in vitro (Hickey and Hochstrasser, 2015). Further experiments suggested that Arg-173 of the homeodomain is part of the surface recognized by Slx5/Slx8. However, the role of the homeodomain in α2 degradation has been only minimally explored until now.

Starting with an unbiased screen for residues of α2 that affect its Ubc4-dependent degradation, we have uncovered a major role for DNA binding in α2 degradation. Mutants of α2 with impaired DNA interaction are not further stabilized by loss of the Ubc4 pathway but are markedly stabilized by loss of the Doa10 pathway; this contrasts with wild-type (WT) α2, for which both pathways need to be inactivated for robust protein stabilization. We propose that DNA binding by WT α2 constrains its localization or mobility within the nucleus, making it less susceptible to Doa10-mediated ubiquitylation at the inner nuclear membrane (INM) and more accessible to the chromatin-associated Slx5/Slx8 enzyme. Therefore, the requirement for two distinct ubiquitylation pathways in α2 degradation appears to reflect the need to access the substrate in different subdomains of the nucleus.

RESULTS

Identification of α2 residues important for its degradation by the STUbL Slx5/Slx8

We have previously utilized reporter constructs fusing a degron to the Ura3 enzyme, allowing stability of the fusion protein to be estimated by the rate of growth on media lacking uracil (Chen *et al.*, 1993; Hickey and Hochstrasser, 2015). A fusion protein encoding α2-Ura3-3HA, where 3HA denotes a C-terminal triple hemagglutinin epitope tag, is targeted by the same two ubiquitylation pathways that target unmodified α2 (unpublished data) (Figure 1A). However, a variant of this fusion protein with two substitutions (I4T, L10S) in *Deg1*, which we call α2*-Ura3-3HA, was shown to be biased toward the Ubc4-Slx5/Slx8 pathway (Xie *et al.*, 2010) (see Figure 1, B and C).

Using a *LEU2*-based plasmid expressing this fusion protein (Figure 1D), we performed a gap-repair screen for mutations that stabilize α2*-Ura3-3HA. Cotransformation of a gapped plasmid expressing this fusion with a PCR product spanning the deleted portion of the plasmid led to homologous recombination between the two DNA molecules. PCR was performed using the intrinsically error-prone Taq polymerase and, in some cases, conditions to enhance its error rate (see *Materials and Methods*). If the transformed yeast grew well on media lacking uracil, which would occur if the mutated α2*-Ura3-3HA protein was resistant to degradation, then we recovered the plasmid and sequenced the α2 open reading frame (ORF). Each unique plasmid was transformed back into yeast to confirm enhanced growth on synthetic defined (SD) uracil compared with yeast carrying the original plasmid expressing α2*-Ura3-3HA. Figure 1E shows a representative growth assay. It compares growth of WT yeast carrying either of two different variant plasmids from the screen to both WT and *slx8*Δ yeast bearing the unmutated input plasmid.

A total of 72 plasmids were sequenced, all of which encoded proteins with at least one amino acid substitution in the α2* portion of the fusion protein (Supplemental Table 1). Strikingly, all plasmids encoding proteins with only one substitution had that mutation within the homeodomain (Figure 1F, group I). Several plasmids encoded proteins with substitutions that were found singly but also included mutations not found singly (Figure 1F, group II). A third group of plasmids encoded proteins with multiple substitutions, none of which were found singly in the screen (Figure 1F, group III). The presence of mutations throughout the α2* gene in the collection of plasmids recovered from the screen, which also included silent mutations, indicated that the mutagenesis by error-prone PCR was not limited to any region of the α2 ORF. However, some bias toward certain regions of the ORF cannot be ruled out. Supplemental Table 1 lists all nucleotide and amino acid changes for each sequenced plasmid.

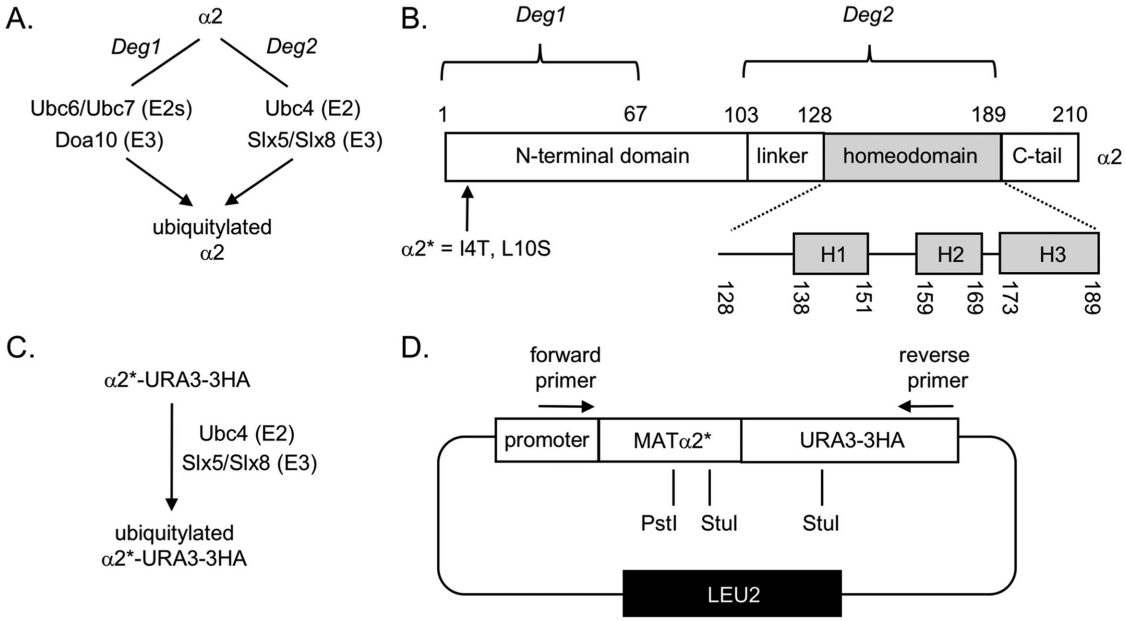

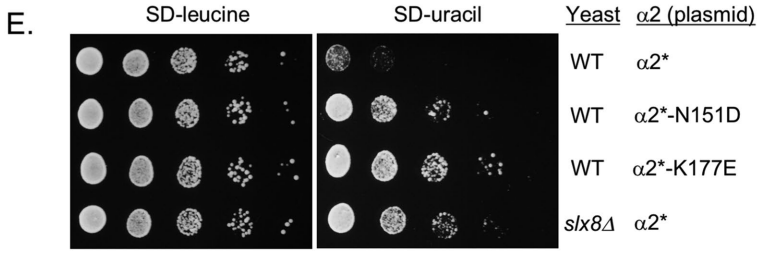

F.

Group I.		Group II.	Group III.
R135Q	L171F	I67T, L144P	K63R, L171S
R135W	I176T	W179C, K186E	R173W, K208R
R135L	K177E	A149T, R183G	V115E, R173L
F136S	W179G	V141E, I174V	N64D, W147G
V141E	V180G	R135Q, I192N	V119A, V180D
L144P	S181P	V141E, N182K	R173L, N182I
E145G	N182D	K160N, I176T	V87G, V180D
W147R	R183G	F136V, V141E	F116L, Q121H, W179C
F148S	R184G	V119G, F148S	T137A, W179R, E210D
F148C	R184S	K129N, T169A	Y156H, N182I
N151D	R185G	D53A, F136Y, N151D	R99K, V180D
T169A	K186E	N168D, K177E	N62Y, Q175P, K208E
T169I	K186I		
L171V			

FIGURE 1: Screen for mutations in α2 that affect its STUbL-mediated degradation. (A) Schematic summarizing the ubiquitylation of α2. *Deg1* and *Deg2* are previously characterized degrons in α2. (B) Diagram of the domain organization of α2. The homeodomain is cartooned in more detail, with helices (H1, H2, and H3) shown as gray bars. Numbers indicate the amino acid boundaries of the different domains or helices. (C) Schematic depicting ubiquitylation of the α2*-Ura3-3HA protein, which contains I4T and L10S mutations in α2 (indicated by *) that were previously shown to bias its degradation to the Ubc4/Slx5/Slx8-pathway. (D) Diagram of the plasmid used in the screen to identify residues that stabilize α2*-URA3-3HA. The pJM130-α2*-URA3-3HA plasmid was cut with *Pst*I and *Stu*I and then transformed into yeast MHY501 along with DNA amplified by PCR from the same plasmid using primers cmh100 (forward) and cmh105 (reverse). (E) Assay for growth on media lacking leucine or uracil following 10-fold serial dilution. Growth rate on media lacking uracil is dependent on the levels of the α2*-URA3-3HA fusion protein. Plasmids expressing the indicated version of α2*-URA3-3HA were transformed into either WT (BY4741) or *slx8*Δ (MHY4203) yeast, as indicated. (F) Mutations found in plasmids from the screen depicted in D. Mutations listed in group I are those with a single amino acid change. Mutants in group II are those in which an amino acid change found singly (listed in group I; underlined in group II) was accompanied by at least one other additional amino acid change. Mutants in group III had amino acid alterations that were not found singly.

All of the amino acid substitutions found singly in the screen—and others that were not found singly—are predicted to disrupt DNA binding by the homeodomain. A published high-resolution structure of the α2 homeodomain bound to its site-specific DNA revealed the α2 residues directly involved in DNA interaction, most notably Arg-135, Ser-181, Asn-182, and Arg-185 (Figure 2A)

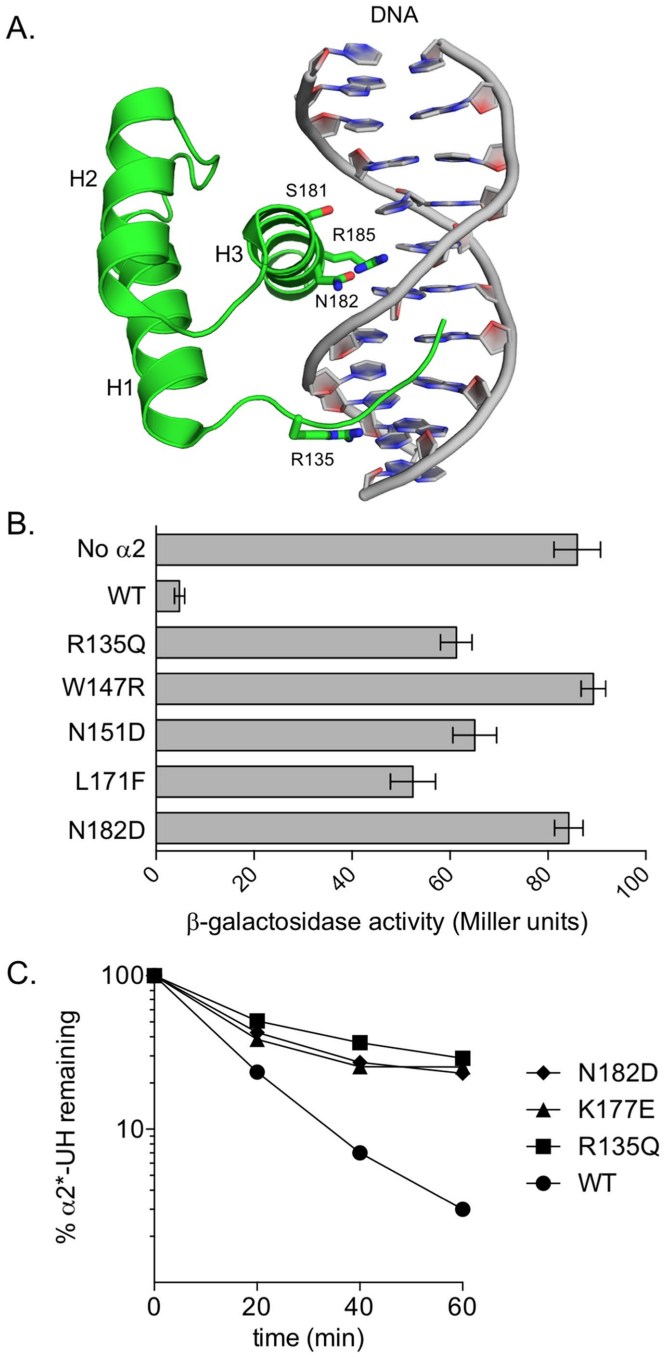

FIGURE 2: Role for α2 DNA binding in the STUbL pathway of α2 degradation. (A) Crystal structure of the α2 homeodomain (green) bound to operator DNA. Helices (H1, H2, H3) and select residues in α2 crucial for DNA interaction are indicated. PDB code: 1APL. Image rendered using Pymol, with expert assistance provided by Judith Ronau. (B) Assay for repression of a-specific gene transcription in MHY481 cells by α2 or the indicated variant, expressed from plasmid pJM130. Error bars represent SD ($N = 3$). (C) Radioactive pulse-chase analysis of α2*-URA3-3HA or the indicated variant, expressed from a p414MET25-based plasmid, in *matα2Δ* cells (MHY1147).

(Wolberger *et al.*, 1991). Substitutions of these and other residues were later shown to impair interaction of α2 with DNA (Vershon *et al.*, 1995). Examination of the structure of α2 bound to DNA also predicts that several of the mutations found in our screen are likely to disrupt the structure of the homeodomain, indirectly impairing its interaction with DNA. These mutations include likely helix breakers of helix 1 (L144P, E145G) and helix 3 (Q175P, W179G, V180G, S181P, R183G, R184G, R185G). In addition, mutation of residues buried within the core of the homeodomain (W147, F148, N151, I176, T169, L171, W179, V180) are predicted to disrupt packing of the helices involved in DNA recognition. Indeed, using an established assay of a-specific gene (asg) repression involving the *Escherichia coli lacZ* gene under control of an asg operator (Vershon *et al.*, 1995; Hickey and Hochstrasser, 2015), each of the mutations tested disrupted the ability of α2 to repress transcription (Figure 2B and unpublished data).

Noteworthy among the plasmids with multiple mutations in α2* are those encoding proteins with mutations at the Arg-173 position, which we previously showed is important for Slx5/Slx8-mediated ubiquitylation of α2 (Hickey and Hochstrasser, 2015). While no substitutions at Arg-173 were found singly in the screen, we subsequently showed that either α2*(R173L)-Ura3-3HA or α2*(R173W)-Ura3-3HA yielded significantly enhanced yeast growth on SD-uracil compared with α2*-Ura3-3HA (Supplemental Figure 1A). Arg-173 is surface exposed but does not make direct contact with DNA (Wolberger *et al.*, 1991). An R173A mutant is known to have normal DNA interaction but be impaired for interaction with the corepressor Ssn6 (Smith and Johnson, 2000). Consistent with this, multiple substitutions at Arg-173 partially reduced a-specific gene repression (Smith and Johnson, 2000) (Supplemental Figure 1B).

Since the growth assay on SD-uracil is only an indirect measure of protein stability, we employed radioactive pulse-chase assays to determine whether the mutated α2*-Ura3-3HA proteins were indeed more metabolically stable. For these analyses, we selected variants with mutations in surface-exposed residues known to make direct contact with DNA over those likely to disrupt the homeodomain fold. We analyzed mutations in two distinct regions of the homeodomain: the unstructured N-terminal arm, which contacts the DNA minor groove (R135Q), and helix 3 (also called the recognition helix), which contacts the major groove (K177E and N182D). All three mutations inhibited degradation of the α2*-Ura3-3HA protein (Figure 2C). Thus, mutating the DNA-binding interface of an α2 derivative that is targeted for degradation through *Deg2* and the STUbL pathway interferes with its turnover.

A previously characterized α2 DNA-binding mutant is strongly stabilized

We next determined whether mutants of otherwise-unaltered, full-length α2 with reduced DNA interaction have altered degradation kinetics in cells. For this, we began with a set of α2 variants that were already characterized for their ability to bind DNA both in vivo and in vitro (Vershon *et al.*, 1995). The α2(S181A, N182A, R185A) mutant (α2-3Ala), in which three residues within the recognition helix of the homeodomain (Figure 2A) are changed to alanines, had a strikingly slow degradation rate compared with WT α2 and other DNA binding mutants (Figure 3B). The three residues mutated in the α2-3Ala mutant make direct contact with DNA and mutation of each of these residues singly impairs DNA interaction (Wolberger *et al.*, 1991; Vershon *et al.*, 1995). However, alanine substitution for any of these three residues alone did not result in significant stabilization of α2 (unpublished data and Supplemental Figure 4).

These results were surprising. On the one hand, the expected correlation between α2 DNA binding and degradation suggested from the screen in Figure 1 was not observed. On the other hand, α2-3Ala was remarkably stable for a protein that still contained an

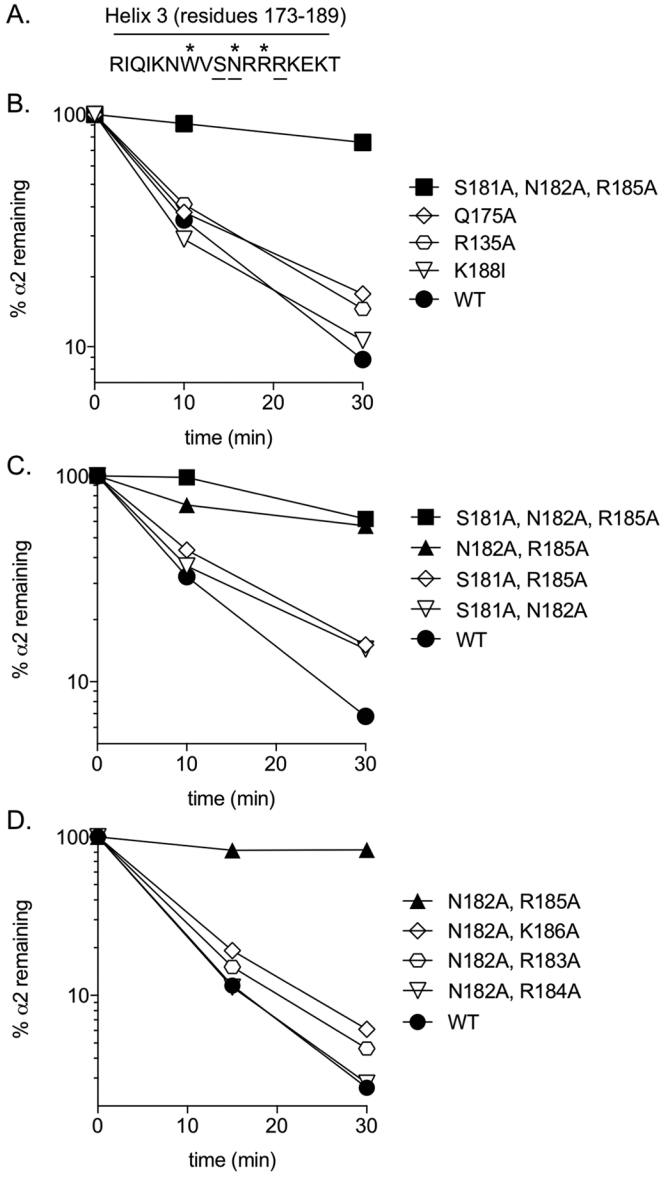

FIGURE 3: While most DNA binding mutants of otherwise WT α2 are not stabilized, a specific double alanine mutant is very stable. (A) The amino acid sequence of the recognition helix (helix 3) within the α2 homeodomain is displayed. Underlined residues are those mutated to alanine in the α2(S181A, N182A, R185A) mutant. Residues that are conserved in nearly all homeodomains are marked with an asterisk. (B) Radioactive pulse-chase analysis of α2 or the indicated α2 variant, selected from a previously characterized panel of mutants (Vershon *et al.*, 1995). Plasmids (pAV115-based) expressing the indicated α2 were transformed into *matα2Δ* cells (MHY2622). (C) Pulse-chase analysis of α2 or the indicated α2 variant. Plasmids (pAV115-based) expressing the indicated α2 were transformed into *matα2Δ* cells (MHY2622). (D) Pulse-chase analysis of α2 or the indicated α2 variant. Plasmids (pRS314-based) expressing the indicated α2 were transformed into *matα2Δ* cells (MHY1147). Protein turnover experiments in this figure were performed only once; however, turnover for many of these α2 variants was tested as part of other experiments (see subsequent figures and unpublished data). Slow turnover for the α2(S181A, N182A, R185A) and α2(N182A, R185A) variants was consistently observed in several experiments.

intact *Deg1* degron, unlike the still relatively rapid degradation of α2 bearing other *Deg2* mutations.

We examined this unanticipated stabilization more closely by testing all possible two-residue mutant subsets of α2-3Ala. A double substitution mutant of α2 in which Asn182 and Arg185 were mutated to alanine was as long lived as α2-3Ala (Figure 3C). By contrast, the other two possible double mutants were only marginally more stable than WT α2. Notably, Asn182 is nearly invariant across homeodomains, always hydrogen bonding to an adenine base of DNA (Figure 2A) (Wolberger *et al.*, 1991; Burglin and Affolter, 2016). Other residues in helix 3 are also involved in DNA binding. We tested whether mutation of Asn182 to alanine as part of other double alanine substitution mutants of helix 3 would give similar effects as the α2(N182A, R185A) mutant. This was not the case (Figure 3D). For instance, the α2(N182A, R184A) mutant, affecting two residues that are nearly invariant across homeodomains, had degradation kinetics identical to those of WT α2 (Figure 3D, open triangles). Thus, the drastic stabilization observed for the α2(N182A, R185A) mutant appears to be very specific, not being observed with any other tested DNA-binding mutants of α2.

Reduction of DNA binding generally does not impair α2 proteolysis

We next asked whether the nature of the mutations at the Asn182 and Arg185 positions was important for the unusual stabilization of α2(N182A, R185A). Interestingly, multiple double-substitution mutants of Asn182 and Arg185 involving residues other than alanine at one of the two positions had normal degradation kinetics (Figure 4A). For example, α2(N182D, R185A), which includes the Asn-182-to-Asp substitution found in our mutant screen using α2*-Ura3-3HA, was degraded similarly to WT α2. A general trend from the panel of double mutants tested was that Asn-182 must be mutated to a nonpolar residue (e.g., alanine, valine, or phenylalanine) for stabilization of α2 (Figure 4A). The residue at position 185 was important as well, but polar residues at this position yielded modestly stabilized proteins (if position 182 was an alanine). Nonpolar residues at both positions led to very strong α2 stabilization.

We addressed the possibility that stabilization of α2 through reduction of DNA binding occurs only when such binding is very severely impaired. We first tested the ability of different α2 DNA-binding mutants to repress a-specific genes. By this assay, the α2(N182D, R185A) mutant, which has a short half-life indistinguishable from that of WT α2, was even less functional than the highly stabilized α2(N182A, R185A) mutant (Figure 4B). This is at odds with the idea that α2 proteins with severely compromised DNA interaction would be stabilized.

The a-specific gene repression assay has two caveats: 1) it does not specifically measure α2-DNA interaction, and 2) α2 protein levels may vary from one variant to another. This second caveat is a particular problem for our studies since α2(N182A, R185A) is very stable and therefore present at higher levels than other α2 variants in vivo (unpublished data). For these reasons, we developed an electrophoretic mobility shift assay (EMSA) using purified recombinant proteins and fluorescently labeled DNA to directly measure α2-DNA interaction. In cells, α2-DNA interaction involves α2-α2 dimerization via its N-terminus and cooperative DNA binding with the Mcm1 protein, with a-specific gene operators consisting of two Mcm1 binding sites flanked by two α2-binding sites. We assayed the direct α2 homeodomain–DNA interaction by using an α2 fragment consisting of the α2 linker, homeodomain, and C-terminal

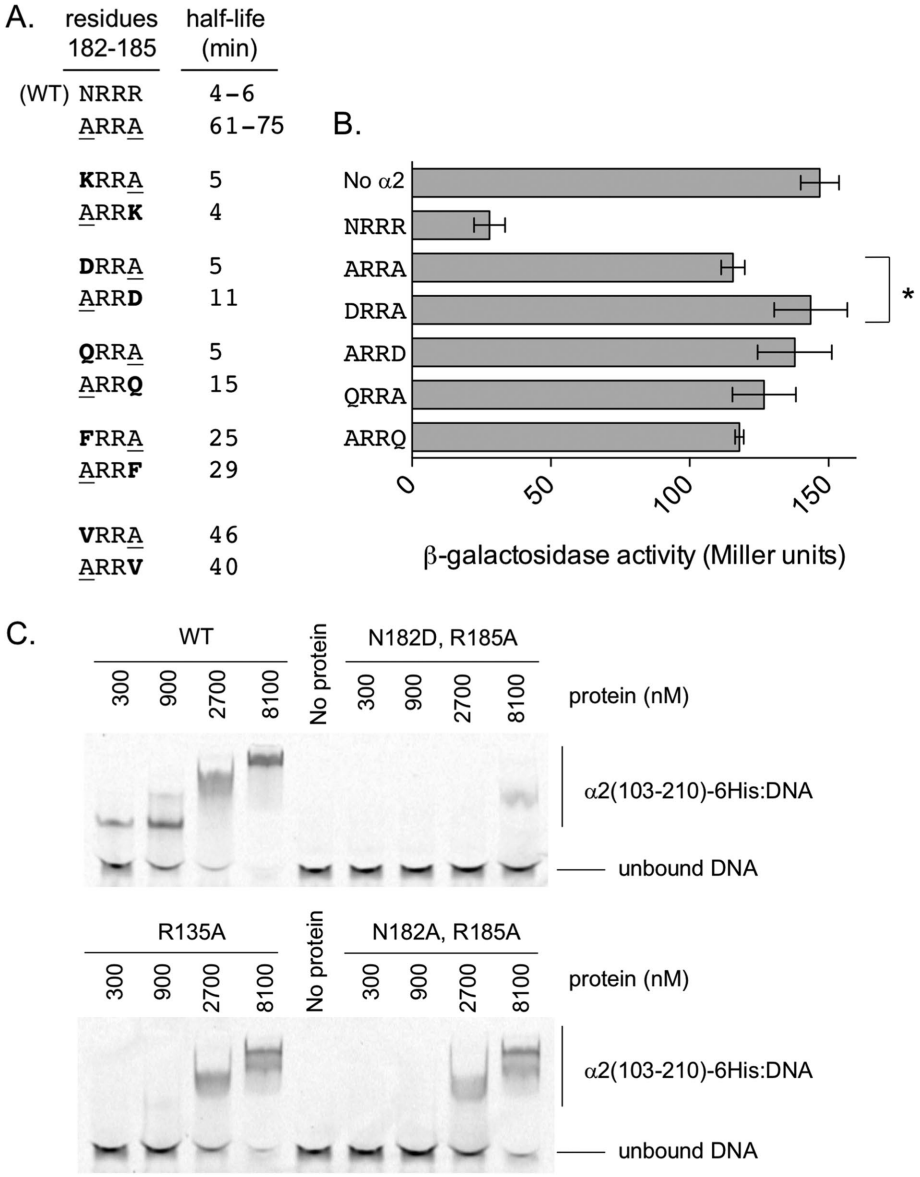

FIGURE 4: Reduced DNA binding is not the sole cause of stabilization for the α2(N182A, R185A) mutant. (A) Degradation rates, reported as half-life, for the indicated α2 variant following pulse-chase analysis in *mat*α2Δ cells (MHY1147) bearing plasmid pRS314-α2 or variant. Half-life ranges shown for α2-WT and the α2(N182A, R185A) mutant are from at least three replicates. All other half-life values are from a single degradation assay in which α2-WT was also tested and had a half-life of 4–6 min. Each α2 variant was tested at least twice with similar results. (B) Assay for repression of a-specific gene transcription in MHY481 cells by α2 or the indicated variant, selected from those characterized in degradation assays (A). Error bars denote SD ($N = 3$). *$p = 0.025$. No other α2 variant tested, besides α2(N182D, R185A), yielded statistically poorer repression than the α2(N182A, R185A) variant. (C) Representative EMSA data for the interaction of purified $\alpha2_{103\text{-}210}$-6His, or the indicated variants of this protein, with synthetic, Cy5-labeled DNA corresponding to regulatory sequence upstream of *BAR1* (an a-specific gene). DNA used was a half operator (a single α2 binding site and single Mcm1 binding site), and no Mcm1 protein was included in assays shown. Two previous experiments, using independent protein preparations, showed comparable DNA binding efficiencies for the different $\alpha2_{103\text{-}210}$-6His variants.

tail and DNA containing a single α2-binding site (Figure 4C). While the $\alpha2_{103\text{-}210}$-6His protein bound DNA well, variants of this protein with mutations in key residues for DNA interaction all had reduced DNA binding. Importantly, however, the $\alpha2_{103\text{-}210}$(N182D, R185A) protein bound DNA significantly less well than the $\alpha2_{103\text{-}210}$(N182A, R185A) protein (Figure 4C), congruent with its more severe gene repression defect in vivo (Figure 4B).

In our EMSAs, all variants except the $\alpha2_{103\text{-}210}$(N182D, R185A) protein caused the majority of the DNA to be to shifted at high protein concentrations (Figure 4C). In contrast, at low protein concentrations, only the WT $\alpha2_{103\text{-}210}$-6His protein resulted in a distinct band corresponding to a 1:1 interaction between $\alpha2_{103\text{-}210}$-6His and DNA. The less mobile protein:DNA species observed at high protein concentrations, even with the WT protein, are presumably due to non-sequence-specific interactions of multiple protein molecules with a single DNA molecule (Vershon and Johnson, 1993). Since these super-shifted species are present using both the $\alpha2_{103\text{-}210}$(N182A, R185A) and $\alpha2_{103\text{-}210}$(R135A) proteins, it is unlikely that a nonsequence-specific DNA binding activity of α2 can explain the strong stabilization of the α2(N182A, R185A) protein. One possibility is that the α2(N182A, R185A) protein, and not the WT or α2(R135A) protein, binds to an unidentified DNA sequence not present in our EMSA assays but present in the yeast genome.

Given the unusual properties of α2(N182A, R185A) and related mutants, we hypothesized that these are gain-of-function mutants, perhaps due to a DNA interaction that does not occur, or is less robust, with WT α2. Asn182 and Arg185 are part of helix 3 of the homeodomain, and helix 3 can still form in the α2-3Ala mutant (Vershon *et al.*, 1995; Ke *et al.*, 2002). Disrupting helix 3, by this model, would interfere with the putative neomorphic DNA-binding activity of α2(N182A, R185A) and may therefore at least partially restore its degradation in vivo. We added predicted helix-breaking mutations, each found in our screen for mutations in α2*-Ura3-3HA (Figure 1). Indeed, substituting Pro or Gly residues at Ser181 or Arg183, respectively, in the context of the α2(N182A, R185A) mutant restored degradation kinetics to WT α2 rates (Figure 5). Thus, it appears that the α2(N182A, R185A) mutant requires an intact DNA-recognition helix for a binding activity not exhibited by normal α2, which shields it from rapid degradation in cells.

We also considered the possibility that the α2(N182A, R185A) mutant would affect degradation and function of WT α2 in the same cell, perhaps by changing the localization of the normal protein. However, this does not seem to be the case, as the presence of α2(N182A, R185A) did not affect the degradation rate of WT α2 or the ability of α2 to repress a-specific genes (Supplemental Figure 2).

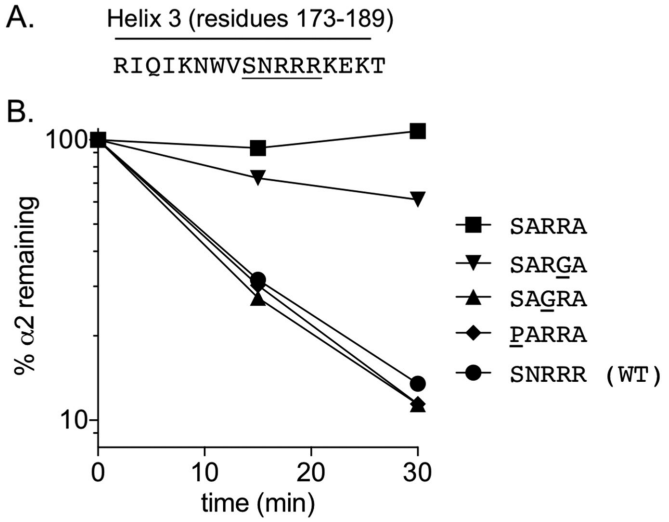

FIGURE 5: Putative helix 3 helix breaker mutations destabilize the α2(N182A, R185A) mutant. (A) The amino acid sequence of the recognition helix (helix 3) within the α2 homeodomain is displayed. (B) Pulse-chase analysis of α2 or the indicated α2 variant. pRS314-based plasmids expressing the indicated α2 were transformed into MHY1147 cells (*matα2Δ*). See Supplemental Figure 5 for additional data on the α2(N182A, R183G, R185A) allele. Turnover of the α2(S181P, N182A, R185A) allele was tested 3 times, with similar results. Turnover of the α2(N182A, R184G, R185A) allele was tested twice, with similar results.

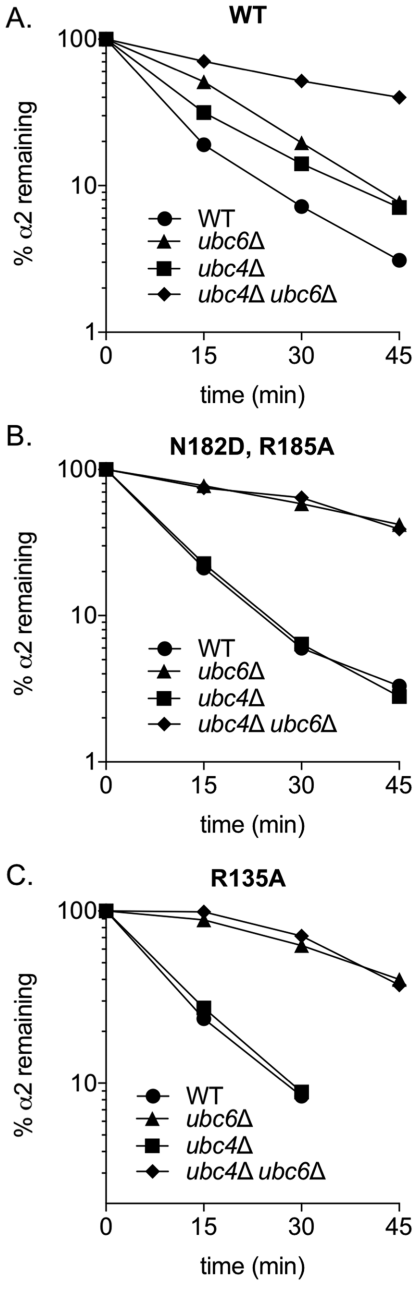

FIGURE 6: DNA binding mutants of α2 are largely substrates of the Doa10 pathway, not the Ubc4 pathway in vivo. Pulse-chase analysis of α2 or the indicated α2 variant, expressed from pRS314-α2 plasmids, in the following strains, as indicated: *matα2Δ* (WT; MHY1147), *matα2Δ ubc4Δ* (MHY1149), *matα2Δ ubc6Δ* (MHY1148), or *matα2Δ ubc4Δ ubc6Δ* (MHY1131). See Supplemental Figure 3 and Figure 10 for additional data on degradation of the α2(R135A) and α2(N182D, R185A) proteins, respectively.

DNA-binding mutants of α2 are largely Doa10 pathway substrates in vivo

Collectively, the data in Figures 3–5 argue that reduction of DNA binding by α2 generally does not impair its proteolysis. For example, the α2(N182D, R185A) mutant had essentially no DNA-binding activity in vitro and was nonfunctional as a transcriptional repressor in vivo (Figure 4, B and C), yet it displayed normal degradation kinetics (Figure 4A). In apparent contradiction to this, our screen for stabilized α2*-URA3-3HA proteins identified numerous DNA-binding mutations (Figure 1).

A hypothesis that might reconcile these findings would be that *Deg2* targeting by the Ubc4-Slx5/Slx8 pathway, which is responsible for most α2*-URA3-3HA turnover, is strongly impaired by loss of substrate-DNA binding, whereas α2 targeting to the Doa10 pathway is potentiated by loss of such binding. We say "potentiated" because simply blocking the Ubc4 pathway in cells where the Doa10 pathway is intact causes an approximately twofold drop in α2 degradation rate (Figure 6A) (Chen *et al.*, 1993). WT α2 is only robustly stabilized when both pathways are disrupted. Strikingly, degradation of the α2(N182D, R185A) mutant was severely impaired in cells lacking only Ubc6 (one of the E2s for the Doa10 pathway) and was not altered at all in cells lacking Ubc4 (Figure 6B). In fact, the degradation rate of α2(N182D, R185A) was as slow in the *ubc6Δ* single mutant as in cells lacking both Ubc6 and Ubc4 (Figure 6B, triangles and diamonds). These epistasis data are consistent with the hypothesis that loss of DNA binding had not only eliminated the ability of the Ubc4-Slx5/Slx8 pathway to target α2 but also allowed the Doa10 pathway by itself to maintain WT rates of α2 degradation.

Further support for this conclusion arose from an analysis of a distinct set of α2 DNA-binding mutants. Several DNA binding-defective mutations affecting Arg135 in the minor groove-contacting N-terminal arm of the homeodomain were isolated in the α2*-URA3-3HA stabilization screen (Figure 1F). By contrast, in the context of full-length and untagged α2, an R135A mutation allowed near-normal degradation kinetics in WT yeast (Figure 3B). As was true of the recognition-helix mutant α2(N182D, R185A), degradation of α2(R135A) was drastically, and similarly, impaired in both *ubc6Δ* cells and *ubc4Δ ubc6Δ* cells (Figure 6C). WT α2 was only modestly stabilized in *ubc6Δ* cells (Supplemental Figure 3), as expected.

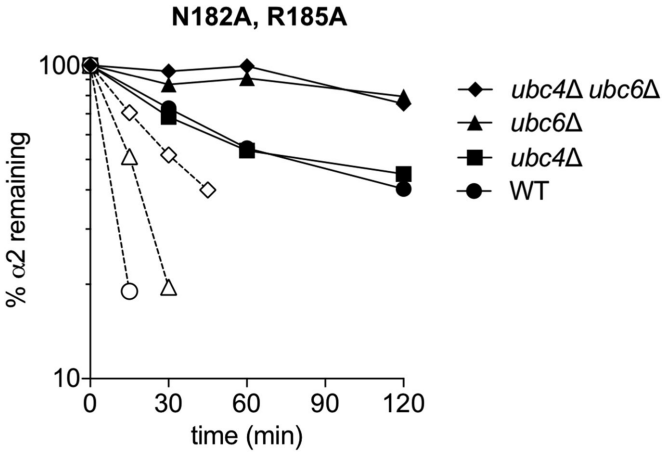

FIGURE 7: Slow degradation of the α2(N182A, R185A) mutant is facilitated by the Doa10 pathway. Pulse-chase analysis of α2(N182A, R185A), expressed from a pRS314-based plasmid in the following strains, as indicated: *matα2Δ* (WT; MHY1147), *matα2Δ ubc4Δ* (MHY1149), *matα2Δ ubc6Δ* (MHY1148), or *matα2Δ ubc4Δ ubc6Δ* (MHY1131). Chase buffer had no cycloheximide in this experiment. Open symbols connected by dashed lines represent degradation of WT α2 (a portion of the same data shown in Figure 6A) for comparison.

In contrast to α2(N182D, R185A), the α2(N182A, R185A) mutant was very stable in WT cells; nevertheless, it did still undergo slow turnover (Figures 3 and 4). We therefore tested whether this residual degradation was dependent on one or both of the pathways that normally target α2 for destruction. As with the more typical, unstable DNA-binding mutants, the slowly degraded α2(N182A, R185A) mutant was targeted mainly by the Ubc6-Ubc7-Doa10 pathway and not the Ubc4-Slx5/Slx8 pathway (Figure 7). Since the single-residue mutants α2(N182A) and α2(R185A) have significant DNA-binding defects on their own (Vershon *et al.*, 1995), we tested degradation of these mutants in the different deletion strains. Again, the DNA binding-defective α2 variants were targeted by the Doa10 pathway and not the Ubc4 pathway (Supplemental Figure 4). However, the rate of degradation for the α2(N185A) mutant in *ubc6Δ* and *ubc4Δ ubc6Δ* cells suggests that additional, unidentified pathways contribute weakly to its degradation. This was also the case with the α2(N182A, R183G, R185A) mutant, in which an alternative recognition helix (due to two alanine substitutions) is likely disrupted by a glycine substitution (Supplemental Figure 5).

Recognition of α2 DNA-binding mutants by Slx5/Slx8 in vitro

Using an in vitro ubiquitylation assay with different fragments of α2, we previously showed that Slx5/Slx8 mainly recognizes the homeodomain of α2 (Hickey and Hochstrasser, 2015). Thus, mutations in the DNA-binding interface may directly or indirectly affect α2 binding by Slx5/Slx8. Indeed, the Arg-173 residue, which was previously suggested to be part of the Slx5/Slx8:α2 interface, is very close to the residues that make direct contact with DNA. Based on the same in vitro assay used in our previous work, two distinct DNA binding mutants of the $\alpha2_{103\text{-}210}$-6His protein showed only modestly reduced ubiquitylation compared with the WT α2 fragment (Figure 8). Thus, it is unlikely that decreased interaction between Slx5/Slx8 and α2 can explain the nearly complete loss of degradation dependence on the Ubc4-Slx5/Slx8 pathway in α2 DNA-binding mutants (Figure 6).

DNA-binding mutants of an α2 homeodomain fragment partially mislocalize to the cytoplasm

The α2 protein has two reported nuclear localization signals (NLSs), one near its N-terminus and the other in the homeodomain (Hall *et al.*, 1990). Consistent with these findings, a fusion of the α2 homeodomain (residues 120–189 in our construct) to green fluorescent protein (GFP) was highly concentrated in the nucleus (Figure 9A). However, whether the homeodomain has a true NLS is unclear. Based on deletion analyses, Hall *et al.* proposed that the homeodomain NLS consists of what is now known to be helix 1 of the homeodomain (Hall *et al.*, 1990; Wolberger *et al.*, 1991). However, deleting helix 1 is likely to disrupt the homeodomain fold; indeed, likely helix-breaking mutations within helix 1 were found in our mutagenesis screen (Figure 1). When we mutated surface-exposed, positively charged side chains (R142 and K150) within helix 1 to inactivate the putative NLS, they caused little change in the localization of the homeodomain-GFP fusion protein (Figure 9A). We conclude that the helix 1 sequence of α2 is unlikely to contain a true NLS.

Instead, DNA binding by the α2 homeodomain may promote its retention in the nucleus. In support of this, DNA-binding mutants of the homoeodomain fusion protein showed significant mislocalization to the cytoplasm, with the α2(N182D, R185A) mutant showing the greatest increase in cytoplasmic staining (Figure 9A). No GFP-containing truncation products were detected for the mutants, and each was expressed at levels similar to those of the WT homeodomain fusion protein (Figure 9B). By contrast, because of the N-terminal NLS, reductions in the ability of full-length α2 to bind DNA are not expected to have large effects on its nuclear localization. Indeed, variants of full-length α2-GFP with DNA-binding mutations were still largely localized to the nucleus (Supplemental Figure 6 and unpublished data). Thus, full-length α2 that cannot bind to DNA is still transported into the nucleus where it is likely ubiquitylated by Doa10 at the INM (Deng and Hochstrasser, 2006).

Interplay of DNA binding and the three known degradation elements in α2

We previously characterized three distinct degradation elements in α2, summarized in Figure 10A (Johnson *et al.*, 1998; Hickey and Hochstrasser, 2015). The *Deg1* degron bears hydrophobic residues in a predicted amphipathic helix that are crucial to *Deg1* functionality (Johnson *et al.*, 1998). For example, an F18S substitution in *Deg1*-URA3 leads to essentially full stabilization of the fusion protein. Although this amphipathic helix also functions as a degradation element in full-length α2, the F18S substitution has only very modest effects on its degradation (Johnson *et al.*, 1998; Hickey and Hochstrasser, 2015). This element becomes much more important in α2 variants with a mutated *Deg2* degron (Hickey and Hochstrasser, 2015). Notably, if the F18S substitution was added to the α2(N182D, R185A) DNA binding-defective mutant, substantial stabilization of the resulting protein was also observed (Figure 10B). This is consistent with full *Deg2* functionality depending on DNA binding.

Although the α2(N182D, R185A) mutant is quite stable in cells lacking the Doa10 pathway, it still undergoes slow degradation mediated by a pathway(s) independent of Ubc4 and Ubc6 (Figure 6B). The *Deg2* degron of α2 has two known degradation elements: a set of consecutive hydrophobic residues in the linker domain and the Arg-173 residue in the homeodomain (Figure 10A). We therefore tested whether these degradation elements still contribute to turnover of the α2(N182D, R185A) mutant. Indeed, addition of either a linker element mutation (LVFNVV to DKDNDD) or the R173E mutation to α2(N182D, R185A) further stabilized the mutant protein in cells also lacking the Doa10 pathway (Figure 10C). Hence, the

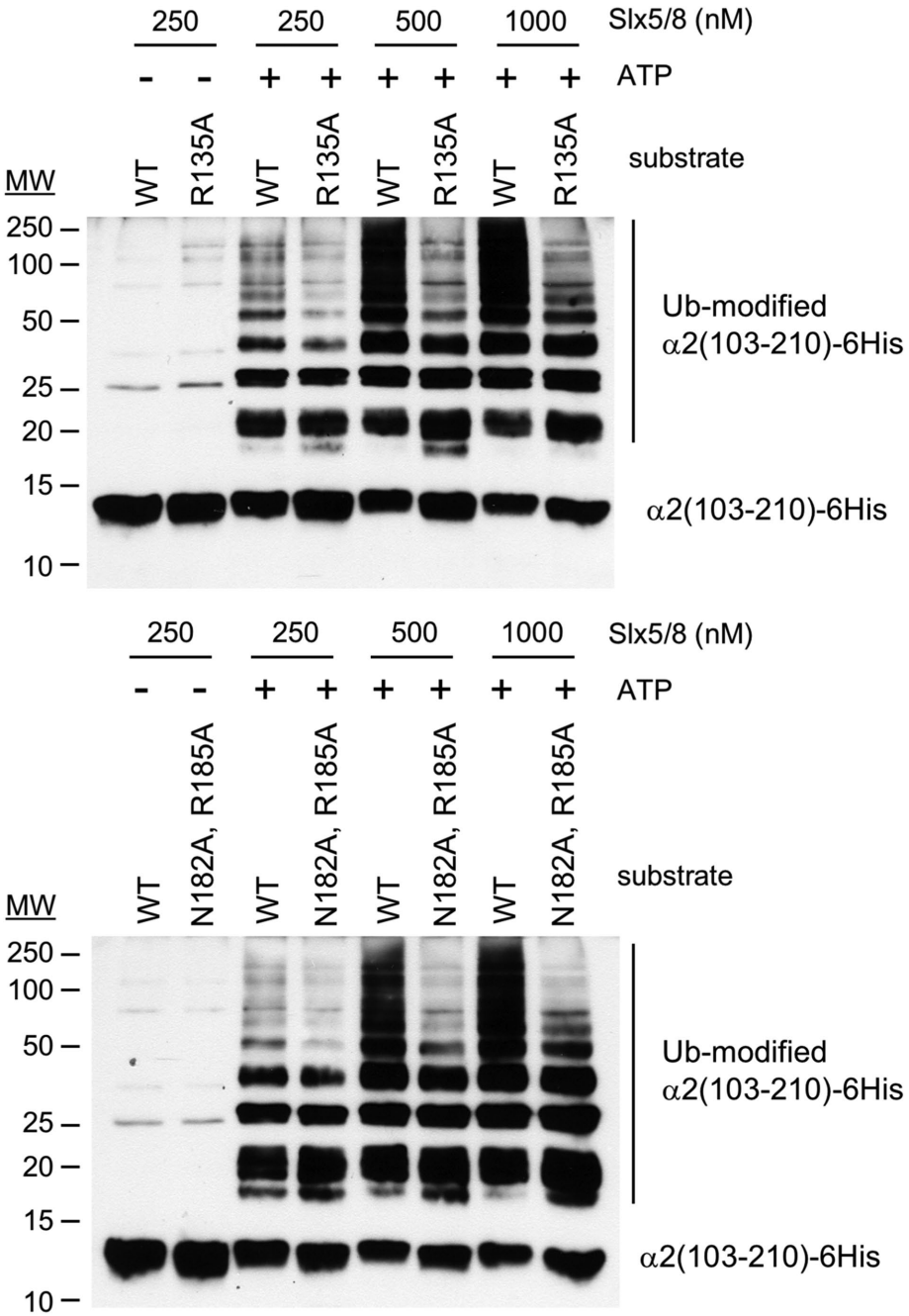

FIGURE 8: DNA-binding mutants of a C-terminal α2 fragment are only slightly defective for ubiquitylation by Slx5/Slx8 in vitro. Slx5/Slx8-dependent in vitro ubiquitylation of $\alpha2_{103\text{-}210}$-6His or the indicated variant. Reactions contained a final concentration of 100 mM NaCl and the indicated concentration of Slx5/Slx8. Reactions were incubated at 30°C for 40 min and stopped by the addition of SDS–PAGE sample buffer followed by heating at 100°C for 6 min. Proteins were separated on a 14% Tris-glycine gel and immunoblotted using anti-α2.

residual Ubc4- and Ubc6-independent degradation of an α2 variant that cannot bind operator DNA also depends on the established degradation elements in *Deg2*.

DISCUSSION

It has long been known that the transcriptional repressor α2 is targeted by at least two ubiquitylation pathways, but the physiological rationale for the involvement of multiple pathways has remained unclear (Chen *et al.*, 1993; Rubenstein and Hochstrasser, 2010). Several other UPS substrates are also targeted by more than one ubiquitylation mechanism (Huyer *et al.*, 2004; Nixon *et al.*, 2010; Hammond-Martel *et al.*, 2012; Cheng *et al.*, 2017). Furthermore, numerous UPS substrates for which a single E3 has been identified are not fully stabilized by inactivation of that E3. Thus, the involvement of multiple ubiquitylation pathways in the degradation of a single UPS substrate may be more common than not.

Sequence-specific transcription factors are often extremely short-lived, and some are known to be targeted by a surprisingly large number of ubiquitylation pathways. For example, in mammalian cells, p53 and Myc were reported to be targeted by at least 12 and six different ubiquitin ligases, respectively (Hammond-Martel *et al.*, 2012; Gonzalez-Prieto *et al.*, 2015). These two UPS substrates might represent extreme examples of multiplex ubiquitin-mediated regulation or might simply be more fully studied because of their central roles in cancer. In the current work, we investigated several mutants of yeast α2 to reveal that α2 degradation by the Ubc4 pathway is dependent on the ability of α2 to interact with DNA (Table 1). In the absence of DNA binding and Ubc4 pathway recognition, α2 is efficiently targeted to the Doa10 pathway. These results are consistent with the fact that inactivation of the Doa10 pathway is sufficient to strongly stabilize proteins bearing just the *Deg1* degron of α2, which does not include any DNA-interaction elements (Swanson *et al.*, 2001). Thus, one rationale for cellular utilization of multiple ubiquitylation pathways is to allow the cell to target distinct subcellular pools of a given protein.

In addition to regulating transcription, Slx5/Slx8 plays multiple roles in genome integrity (Mullen *et al.*, 2001; Zhang *et al.*, 2006; Burgess *et al.*, 2007; van de Pasch *et al.*, 2013). Both subunits localize to the nucleus (Cook *et al.*, 2009). Purified Slx5/Slx8 has weak, nonspecific DNA binding activity, mainly through the Slx8 subunit (Yang *et al.*, 2006). Chromatin association of Slx5/Slx8 is likely also mediated by interaction with other chromatin-bound proteins, in some cases in a SUMO-dependent manner. Like Slx5/Slx8, the human STUbL RNF4 plays numerous roles in genome stability and transcription (Kaiser *et al.*, 2003; Galanty *et al.*, 2012; Yin *et al.*, 2012; Hirota *et al.*, 2014; Wang, 2014; Gonzalez-Prieto *et al.*, 2015), and it also directly interacts with DNA. DNA binding is proposed to contribute to the overall avidity of RNF4 for its chromatin-binding sites, a model supported by the observation that an RNF4 DNA-binding mutant exhibits reduced ubiquitylation of nucleosomal histones (Groocock *et al.*, 2014). Therefore, these STUbLs mainly function in chromatin-associated ubiquitylation. By apparently ubiquitylating the DNA-bound

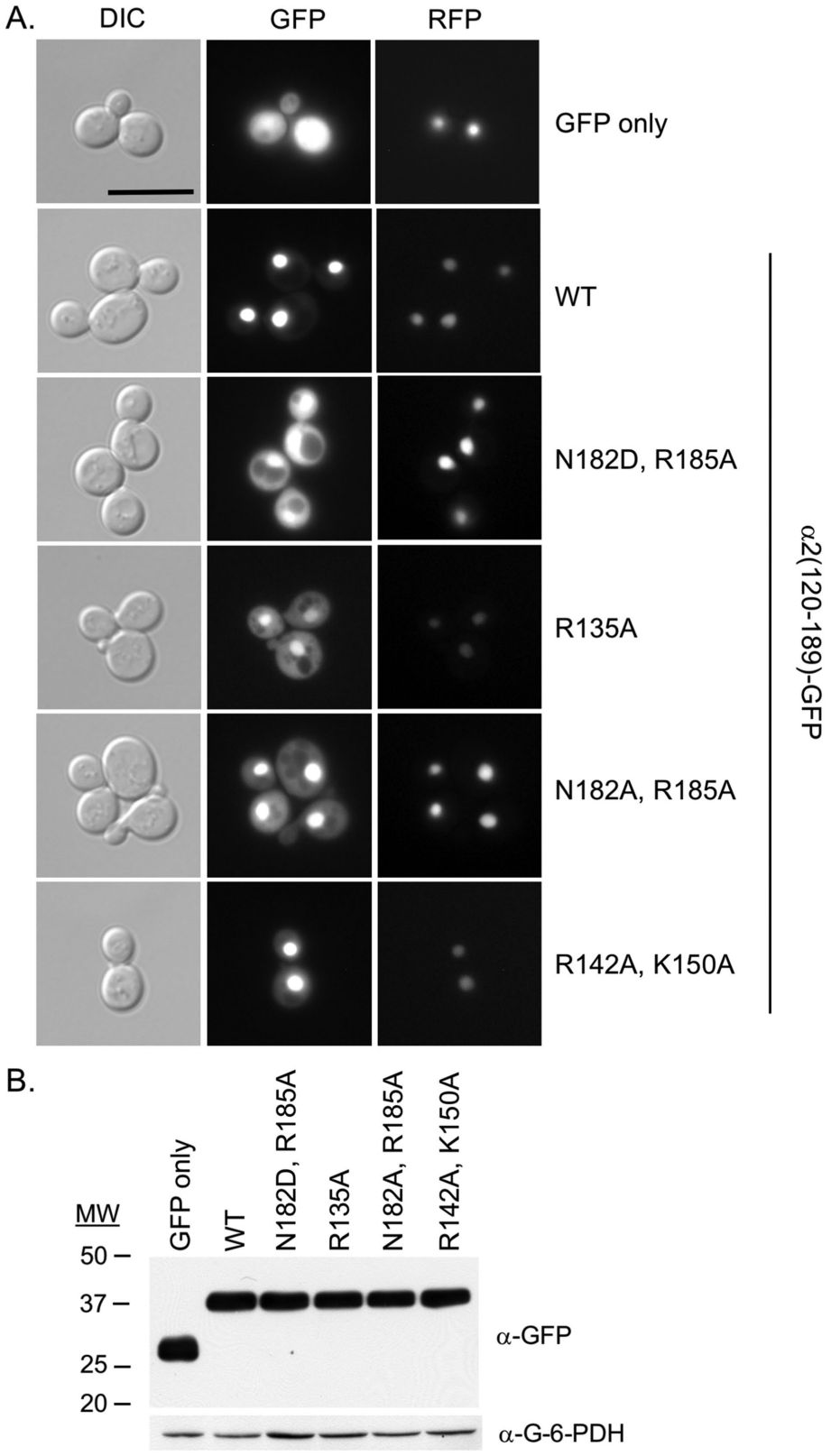

FIGURE 9: Mutants of the α2 homeodomain with reduced DNA interaction have increased localization to the cytoplasm. (A) Representative images showing the subcellular localization of the α2 homeodomain fused to GFP and the indicated mutants of this construct. RFP-Pus1, expressed from a pRS313-NOP1promoter plasmid, served as a nuclear marker. Scale bar = 10 microns. Two previous experiments, using independent yeast transformants but not including the RFP-Pus1 nuclear marker, showed similar localizations for each α2 homeodomain variant. (B) Immunoblot analysis of protein levels for the strains used in A. WT α2(120-189)-GFP was expressed from a p415GPD plasmid, whereas all other GFP fusions were expressed from p415MET25 plasmids. One-half the amount of total cell extract (by cell mass) was loaded for the "GFP only" sample compared with all other samples. GFP-fusions were detected using the JL-8 monoclonal antibody (Clontech). Antibody to glucose-6-phosphate dehydrogenase (G-6-PDH; Sigma) was used as a loading control.

pool of α2, Slx5/Slx8 conforms well to this model (Figures 1 and 6).

DNA binding restricts the mobility of transcription factors in yeast and other species (Karpova *et al.*, 2004; Kumar *et al.*, 2010). Since chromatin is distributed throughout the nucleoplasm with limited dynamics, we predict that α2 variants that cannot bind DNA are more mobile than α2 and therefore more likely to encounter Doa10 at the nuclear periphery. Our data indicate that different DNA-binding mutants of full-length α2 remain primarily in the nucleus (Supplemental Figure 6 and unpublished data), consistent with the presence of an NLS near the N-terminus of α2 (Hall *et al.*, 1990). In contrast, GFP fusions of only the α2 homeodomain bearing the same mutations in its DNA-binding surface mislocalize significantly to the cytoplasm (Figure 9).

Our ubiquitylation data with purified components suggest that mutations in the α2 homeodomain also decrease its direct recognition by Slx5/Slx8 (Figure 8) (Hickey and Hochstrasser, 2015). However, these reductions are unlikely to fully explain the drastic changes in pathway dependence for α2 degradation in vivo. We propose that the α2 DNA-binding mutants become primarily Doa10 pathway substrates for two reasons: 1) they are recognized less well by Slx5/Slx8, and 2) they spend more time at the nuclear periphery due to reduced chromatin association.

Like the homeodomain mutants investigated in the current study, a multi-residue linker domain mutant of α2 is mainly a substrate of the Doa10 pathway and not the Ubc4 pathway (Hickey and Hochstrasser, 2015). However, deletion of *MCM1*, which would also be expected to reduce α2 interaction with DNA upstream of a-specific genes, did not slow α2 degradation in cells also lacking the Doa10 pathway. We have proposed that lack of Mcm1 binding to a WT linker domain exposes a mostly hydrophobic degradation element that is recognized by a component of the UPS (Hickey, 2016). Given that the Ubc4-Slx5/Slx8 pathway mainly operates on chromatin-associated α2 (Figures 1, 2, and 6), α2 may be

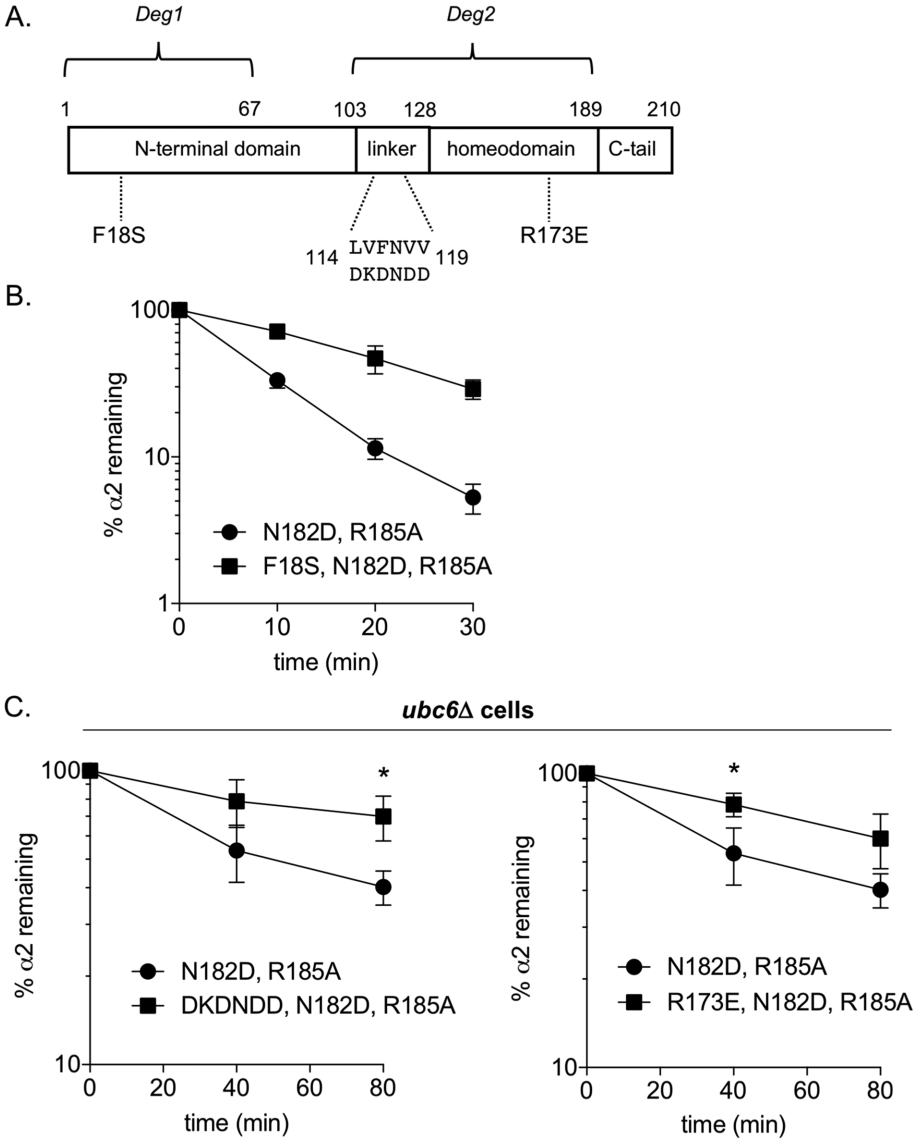

FIGURE 10: The three degradation elements present in α2 remain important for degradation of an α2 DNA binding mutant. (A) Schematic showing the three previously characterized degradation elements of α2. (B) Pulse-chase analysis for the indicated α2 variant, expressed from pRS314-α2 plasmids, in *matα2Δ* (MHY1147) cells. Error bars depict SDs ($N = 3$). (C) Pulse-chase analysis for the indicated α2 variant, expressed from pRS314-α2 plasmids, in *matα2Δ ubc6Δ* (MHY1148) cells. Error bars depict SDs ($N = 3$). Both graphs show the same data for α2(N182D, R185A). *$p < 0.05$ by *t* test using percent α2 remaining at a single timepoint.

targeted by pathways other than the Doa10 or Ubc4 pathways in the absence of Mcm1. *Deg2* fusions, which depend on a WT linker domain, are targeted by the Slx5/Slx8 pathway and another E3 (Hickey and Hochstrasser, unpublished data).

For efficient α-to-a mating-type switching, preexisting α2 must be rapidly inactivated by the ubiquitin system (Laney and Hochstrasser, 2003). Most α2 is DNA bound (Wilcox and Laney, 2009). Here we have shown that DNA binding by α2 in cells specifically limits its access to Doa10 but at the same time is necessary for it to be an efficient substrate for the Slx5/Slx8 pathway. Potentially, a reduction of α2-DNA binding, such as by its posttranslational modification or a global change in chromatin structure, as occurs during mitosis, could reduce α2 targeting to the Slx5/Slx8 pathway, requiring a ubiquitylation pathway that operates on α2 when it is not bound to DNA. Conversely, the Doa10 complex also targets many misfolded protein substrates, particularly those with exposed amphipathic helices and *Deg1* in α2 is predicted to have such a helix (Johnson *et al.*, 1998; Zattas and Hochstrasser, 2015). *Deg1*/α2 might also have direct affinity for membranes, perhaps via its amphipathic helix. This quality control role might overwhelm Doa10 under certain conditions, necessitating alternative means of targeting α2. Thus, distinct α2 ubiquitylation mechanisms could not only provide a way to access α2 in different nuclear subcompartments but may also help cells adapt to changes in either internal or external conditions. Altering the balance of ubiquitylation to one pathway or the other would ensure an efficient switch in mating phenotype.

The α2-3Ala and α2(N182A, R185A) proteins and other α2 variants with nonpolar side chains at positions Asn-182 and Arg-185 are far more stable than WT α2 (Figure 4A). While these mutants are clearly defective in binding a-specific gene operator DNA, our work reveals many other examples of α2 variants with DNA-binding defects in some cases even more severe that display normal degradation kinetics in WT cells (Figures 3 and 4). Therefore, the very stable DNA-binding mutants of α2 such as α2(N182A, R185A) cannot be stabilized solely because of their inability to bind a-specific operator DNA.

The rapidly degraded α2 DNA binding-defective mutants are very effectively targeted by the Doa10 pathway (Figure 6), which is expected given that the *Deg1* degron remains active. However, mutants such as α2(N182A, R185A) also have an intact *Deg1* and are still targeted by the Doa10 pathway, albeit inefficiently (Figure 7), yet they are unusually stable. For these reasons, we believe that these particular α2 DNA-binding mutants gain an interaction that does not occur, or occurs less efficiently, with WT α2, making them less accessible to the Doa10 machinery. Consistent with this gain-of-function hypothesis, the inclusion of residues that are expected to break the presumed third helix of the homeodomain in the α2(N182A, R185A) protein restored normal degradation kinetics (Figure 5). Conceivably, α2(N182A, R185A) and similarly hyperstabilized variants could preferentially localize to a subdomain of the nucleus or sites on DNA that are less accessible to the INM-localized Doa10 complex.

In an interesting potential parallel, the transcription factor p53 is often found mutated to gain-of-function forms in human tumors (Oren and Rotter, 2010). The majority of such p53 mutations are within its DNA-binding domain, and some of the p53 gain-of-function variants are known to bind to alternative DNA sites. Though not completely understood, most p53 gain-of-function mutants are stable proteins, whereas WT p53 is very short lived. Our studies

MATα2 variant	Protein properties	Degradation properties
WT	• Binds specifically to asg DNA	• Rapid • Targeted by two pathways: Doa10 and Ubc4
N182D, R185A	• Impaired binding to asg DNA • Recognition helix is mutated	• Rapid • Targeted mainly by the Doa10 pathway • Unaffected by loss of Ubc4 pathway
R135A	• Impaired binding to asg DNA • Recognition helix is not mutated	• Rapid • Targeted mainly by the Doa10 pathway • Unaffected by loss of Ubc4 pathway
N182A, R185A	• Impaired binding to asg DNA • An alternative recognition helix likely leads to gain-of-function	• Slow • Residual degradation by the Doa10 pathway • Unaffected by loss of Ubc4 pathway
N182A, R183G, R185A	• Impaired binding to asg DNA • The alternative, gain-of-function recognition helix is likely to be disrupted	• Rapid • Targeted mainly by the Doa10 pathway • Mostly unaffected by loss of Ubc4 pathway
N182A	• Impaired binding to asg DNA • Single substitution in recognition helix	• Rapid • Targeted mainly by the Doa10 pathway • Mostly unaffected by loss of Ubc4 pathway
R185A	• Impaired binding to asg DNA • Single substitution in recognition helix	• Rapid • Targeted mainly by the Doa10 pathway • Mostly unaffected by loss of Ubc4 pathway

TABLE 1: Summary of the main MATα2 variants investigated in this study.

indicate such interlinked changes in DNA-binding specificity and protein stability are likely to be widespread among mutated transcription factors, including cases where the changes together induce alterations in cell division and growth.

MATERIALS AND METHODS

Strains and plasmids

All yeast strains used in this study have been described previously and are listed in Supplemental Table 2. Construction of the pJM130-α2*-Ura3-3HA plasmid (α2* carries the *Deg1*-inhibiting I4T and L10S mutations) was previously described (Xie *et al.*, 2010). Plasmids pJM130 and pAV115, and selected variants of these plasmids expressing mutants of α2, were a generous gift from Andrew Vershon (Vershon *et al.*, 1995; Mead *et al.*, 1996). To make plasmid p414MET25-α2*-Ura3-3HA and variants thereof, DNA fragments comprising the *α2** ORF and most of the *URA3* ORF were PCR amplified from pJM130-α2*-Ura3-3HA plasmids using primers cmh675 (5′- GCGCACTAGTATGAATAAAACACCCATTAAAGATC-3′), which includes a *Spe*I site, and cmh105 (5′-GCTGGCCGCATCTTCTCAAATATGCTTCCCAGCCTGCTTTTCTG-3′). The PCR products were digested with *Spe*I and *Nco*I (which cuts near the beginning of the URA3 ORF) and cloned into plasmid p414MET25-α2(103-189)-URA3-3HA that had been digested with *Nco*I and *Spe*I, which cuts just after the MET25 promoter (Hickey and Hochstrasser, 2015).

Plasmids pRS314-α2, p416-α2promoter-α2-FLAG-6His, pET21a-α2(103-210)-6His and selected variants of these plasmids were described previously (Hickey and Hochstrasser, 2015). Additional mutated versions of pAV115, pJM130, pRS314-α2, or pET21a-α2(103-210)-6His were made by subcloning from mutant pJM130-α2*-Ura3-3HA plasmids or by site-directed mutagenesis (Zheng *et al.*, 2004). Plasmids expressing α2-GFP or α2(120-189)-GFP were constructed by amplification of the GFP ORF from pFA6a-GFP(S65T)-kanMX6 and cloning this DNA fragment between the *Hin*dIII and *Xho*I sites of the previously described p415MET25-α2-URA3-3HA and p415MET25-α2(120-189)-URA3-3HA plasmids, respectively, thereby replacing the URA3-3HA cassette with GFP (Longtine *et al.*, 1998; Hickey and Hochstrasser, 2015). A plasmid expressing only GFP was similarly constructed from p415MET25-URA3-3HA, which lacks *α2* sequences (Hickey and Hochstrasser, 2015). For expression of WT α2(120-189)-GFP, the *MET25* promoter in p415MET25-α2(120-189)-GFP was replaced by the GPD (*TDH3*) promoter via subcloning (Mumberg *et al.*, 1995). Plasmid pRS313-RFP-PUS1 was a generous gift from Symeon Siniossoglou (Han *et al.*, 2007).

Yeast growth

Yeast were grown in YPD (1% yeast extract, 2% peptone, and 2% dextrose; all from BD Difco), a minimal rich media, or a SD media. SD media contained 0.67% yeast nitrogen base without amino acids (BD Difco), 2% dextrose, 0.002% adenine (Sigma), 0.004% uracil (Sigma), and the amino acids (all from Sigma) arginine (4 mg/l), histidine (2 mg/l), isoleucine (12 mg/l), leucine (12 mg/l), lysine (8 mg/l), methionine (2 mg/l), phenylalanine (12 mg/l), threonine (10 mg/l), and tryptophan (8 mg/l). Minimal rich media was SD plus 0.5% casamino acids (BD Difco). To select for plasmid maintenance, SD or minimal rich media lacking one or more of the amino acids and/or uracil was used.

Yeast protein degradation assays

For radioactive pulse-chase experiments, 10 OD_{600}-ml equivalents of yeast cells were grown in SD or minimal rich media to logarithmic phase. Cells were harvested by centrifugation in a 15-ml capacity tube and washed twice with 1 ml of SD media lacking all amino acids that had been warmed to 30°C; the culture was transferred to a 2-ml screw-cap microcentrifuge tube during the first wash. Washed cells were then resuspended in 0.2 ml SD media lacking the amino acid methionine. A volume of EXPRE^{35}S^{35}S protein labeling mix (Perkin Elmer; NEG072007MC) yielding ~0.1 mCi of ^{35}S was then added, and cells were vortexed for 10 s and then incubated at 30°C for 6–10 min. Labeled cells were harvested by centrifugation and

resuspended in 0.45 ml of chase buffer (SD media plus 10 mM excess methionine) with 0.5 mg/ml cycloheximide (except where noted in figure legends). A 0.1-ml aliquot was immediately taken as timepoint zero, added to 0.1 ml of 2× lysis buffer (90 mM HEPES, pH 7.5, 2% SDS, 30 mM dithiothreitol [DTT]), and placed on ice until the end of the chase. Subsequent timepoints were collected in the same manner. At the end of the chase, all samples were boiled for 8 min and then frozen at -80°C. Samples were thawed, 1 ml of Triton lysis buffer (50 mM HEPES, pH 7.5, 150 mM NaCl, 5 mM EDTA, 1% Triton X-100) was added, and the tubes were vortexed for 20 s. Samples were clarified by centrifugation at 21,130 × *g* (Eppendorf 5424) for 10 min, and the supernatant was transferred to fresh microcentrifuge tubes. Aliquots of each sample were spotted on filter paper to quantify trichloroacetic acid–precipitable radioactivity, and these values were used to add equivalent amounts of total radioactive protein to fresh microcentrifuge tubes. Polyclonal rabbit antibody to MATalpha2 or monoclonal mouse antibody to the HA epitope (Sigma) was added and samples were incubated at 4°C for 2 h with mixing. Samples were then mixed with Protein A resin (for rabbit antibodies; Repligen) or Protein G resin (for mouse antibodies; Santa Cruz) and incubated at 4°C for 1 h with mixing. Samples were washed four to five times with immunoprecipitation wash buffer (30 mM HEPES, pH 7.5, 150 mM NaCl, 5 mM EDTA, 0.2% Triton X-100, 0.1% SDS) before proteins were eluted by adding 0.06 ml SDS–PAGE sample buffer (50 mM Tris, pH 6.8, 10% glycerol, 2% SDS, 143 mM β-mercaptoethanol, and bromophenol blue to color) and boiling for 5 min. Samples (approximately one-half of each eluate) were subjected to SDS–PAGE, gels were fixed and dried, and the dried gels were exposed to a phosphoimager screen for 1–3 d. Screens were imaged on a STORM860 (GE, Marlborough, MA), and data were analyzed using ImageQuant 5.2 software (GE).

Cycloheximide-chase experiments were carried out as previously described (Hickey and Hochstrasser, 2015). Independent yeast transformants were used for replication of all protein degradation experiments.

Other biochemical methods

The a-specific gene repression assay was performed as reported (Hickey and Hochstrasser, 2015), except that the temperature was 21°C (instead of 30°C) for the experiments in Figure 2B. Independent yeast transformants were used for replication of all a-specific gene repression experiments. In vitro ubiquitylation assays with purified proteins were carried out as previously described (Hickey and Hochstrasser, 2015).

Generation and screening of mutated plasmids by error-prone PCR and gap repair

Approximately 1 µg of pJM130-α2*-Ura3-3HA plasmid DNA was incubated with restriction enzymes *Pst*I and *Stu*I (New England Biolabs) in buffer NEB3.1 for 3 h at 37°C. The reaction was then incubated at 80°C for 20 min to inactivate the restriction enzymes. The linearized DNA (5% of the above digestion reaction) was used to transform WT yeast MHY501, with or without a PCR product amplified from pJM130-α2*-Ura3-3HA. Amplification was catalyzed by Taq polymerase using forward primer cmh100 (5′-GATTGAAATCAGCTTAGAAGTGGGCA-AGAAAAAAAGGAAGATAAGC-3′) and reverse primer cmh105 (see above), which anneal in the α2 promoter and *URA3* ORF, respectively (Figure 1D). PCRs used either standard buffer (20 mM Tris, pH 8.5, 50 mM KCl, 1.5 mM $MgCl_2$, 0.2 mM dNTPs; PCR1) or an error-prone buffer (20 mM Tris, pH 8.5, 50 mM KCl, 7.5 mM $MgCl_2$, 0.2 mM dGTPs and dATP, 1 mM dTTP and dCTP; PCRs 2 and 3). The total volume for each PCR was 0.4 ml, which was divided evenly in 20 PCR tubes before thermal cycling. After thermal cycling, all 0.4 ml was applied to a PCR purification column and processed according to the manufacturer's protocol (Qiagen). The entire eluate was digested with *Hin*dIII in NEB2.1 at 37°C for 1 h (to digest any template plasmid) and then incubated at 80°C for 20 min to inactivate *Hin*dIII before use in yeast transformation reactions.

Yeast transformations used the lithium acetate method (Gietz and Woods, 2002). Logarithmically growing (in YPD) yeast strain MHY501 (50 ml) was washed in 5 ml of 0.1 M lithium acetate, resuspended in 0.25 ml of 0.1 M lithium acetate, and divided among five microfuge tubes. Linearized plasmid and PCR product described above were added as appropriate. Approximately 10-fold more colonies emerged on SD-leucine plates from transformations that included both the linearized plasmid and the PCR product compared with those that only included the linearized plasmid. Colonies that emerged on SD-leucine were replica plated to SD-uracil agar plates. Rapidly growing ura+ colonies (2–3 d at 30°C) were observed only if the PCR product was included in the transformation step. These colonies were picked and grown to saturation in selective liquid medium. Cells were pelleted by centrifugation and lysed using glass beads (Sigma G8772) in a FastPrep (MP Biomedicals), and total DNA was isolated. Plasmids were recovered by electrotransformation (Gene Pulser; BioRad) of this DNA into *E. coli*, with selection on lysogeny broth plates supplemented with ampicillin. The screen was repeated three times, with the first PCR using standard buffer and the second and third PCRs using "error-prone" buffer. Many of the stabilizing mutations were found in more than one replicate of the screen, and the K177E mutation was found in all three replicates; see Supplemental Table 1 for more details.

Electrophoretic mobility shift assays

All EMSA experiments used the $\alpha2_{103\text{-}210}$-6His protein or variants with the indicated amino acid substitutions, the purification of which has been described (Hickey and Hochstrasser, 2015). An oligonucleotide with the sequence 5′-GCTGAAACATGGCATGTAATTACCG-TAAAAGG-3′ and its reverse complement were synthesized and modified at their 5′ ends with Cy5 by Integrated DNA Technologies. The two oligonucleotides were resuspended in annealing buffer (50 mM Tris-Cl, pH 8, 50 mM NaCl, 1 mM EDTA) and annealed by incubation in a thermal cycler: 94° for 4 min, 1 min at each temperature descending to 55°C, 30 min at 55°C, and 1 min at each temperature descending to 25°C. Annealing was verified by electrophoretic mobility shift compared with nonannealed oligonucleotides on a 9% native-PAGE gel (90 mM Tris-borate, 2.5% sucrose, 9% acrylamide 0.31% bis-acrylamide, polymerized with ammonium persulfate and tetramethylethylenediamine) with 90 mM Tris-borate as running buffer. This duplex DNA includes one α2 binding site and one Mcm1 binding site from the regulatory region upstream of the *BAR1* gene. To perform EMSA assays, the indicated $\alpha2_{103\text{-}210}$-6His protein was mixed with 5 nM DNA in EMSA buffer (20 mM HEPES, pH 8, 5 mM $MgCl_2$, 2.5% sucrose, 0.001% Triton X-100, 2 mM DTT) and incubated at 21°C for 1.5 h. Sheared salmon sperm DNA (Worthington, 1440), which was annealed prior to use, was added at 10 mg/l as a nonspecific DNA. Samples were loaded on a 9 or 10% native-PAGE gel (see above) and run for 45 min at 100 V. Gels were imaged wet on a STORM 860 imager (GE) using the red fluorescence mode.

Microscopy

MHY501 or MHY503 cells were transformed with low-copy plasmids expressing fluorescent proteins. WT α2(120-189)-GFP expressed from the MET25 promoter was slightly less abundant than variants of this protein expressed from the same promoter (unpublished

data). Therefore, WT α2(120-189)-GFP was expressed from the GPD promoter for the data shown. Cells were grown in synthetic-defined media to logarithmic-phase, spotted on glass slides, and covered with glass coverslips. All images were obtained using an Axioskop epifluorescence microscope (Carl Zeiss, Thornwood, NY) with a 100× oil objective (1.4 NA), an AxioCam MRm camera (Carl Zeiss), and AxioVision software. Fluorescent images were captured using autoexposure. Images were cropped and intensity levels were adjusted using Photoshop (Adobe).

ACKNOWLEDGMENTS

We thank Jason Berk and Judith Ronau (Yale University) for comments on the article. We thank Andrew Vershon (Rutgers University) and Symeon Siniossoglou (Cambridge Institute for Medical Research, UK) for plasmids. This work was supported by National Institutes of Health grants GM046904 and GM053756 (to M.H.) and F32 GM097794 (to C.M.H.).

REFERENCES

Abed M, Barry KC, Kenyagin D, Koltun B, Phippen TM, Delrow JJ, Parkhurst SM, Orian A (2011). Degringolade, a SUMO-targeted ubiquitin ligase, inhibits Hairy/Groucho-mediated repression. EMBO J 30, 1289–1301.

Burgess RC, Rahman S, Lisby M, Rothstein R, Zhao X (2007). The Slx5-Slx8 complex affects sumoylation of DNA repair proteins and negatively regulates recombination. Mol Cell Biol 27, 6153–6162.

Burglin TR, Affolter M (2016). Homeodomain proteins: an update. Chromosoma 125, 497–521.

Chen P, Johnson P, Sommer T, Jentsch S, Hochstrasser M (1993). Multiple ubiquitin-conjugating enzymes participate in the in vivo degradation of the yeast MAT alpha 2 repressor. Cell 74, 357–369.

Cheng H, Bao X, Gan X, Luo S, Rao H (2017). Multiple E3s promote the degradation of histone H3 variant Cse4. Sci Rep 7, 8565.

Cook CE, Hochstrasser M, Kerscher O (2009). The SUMO-targeted ubiquitin ligase subunit Slx5 resides in nuclear foci and at sites of DNA breaks. Cell Cycle 8, 1080–1089.

Deng M, Hochstrasser M (2006). Spatially regulated ubiquitin ligation by an ER/nuclear membrane ligase. Nature 443, 827–831.

Galanty Y, Belotserkovskaya R, Coates J, Jackson SP (2012). RNF4, a SUMO-targeted ubiquitin E3 ligase, promotes DNA double-strand break repair. Genes Dev 26, 1179–1195.

Geng F, Wenzel S, Tansey WP (2012). Ubiquitin and proteasomes in transcription. Annu Rev Biochem 81, 177–201.

Gietz RD, Woods RA (2002). Transformation of yeast by lithium acetate/single-stranded carrier DNA/polyethylene glycol method. Methods Enzymol 350, 87–96.

Gonzalez-Prieto R, Cuijpers SA, Kumar R, Hendriks IA, Vertegaal AC (2015). c-Myc is targeted to the proteasome for degradation in a SUMOylation-dependent manner, regulated by PIAS1, SENP7 and RNF4. Cell Cycle 14, 1859–1872.

Groocock LM, Nie M, Prudden J, Moiani D, Wang T, Cheltsov A, Rambo RP, Arvai AS, Hitomi C, Tainer JA, *et al.* (2014). RNF4 interacts with both SUMO and nucleosomes to promote the DNA damage response. EMBO Rep 15, 601–608.

Haber JE (2012). Mating-type genes and MAT switching in Saccharomyces cerevisiae. Genetics 191, 33–64.

Hall MN, Craik C, Hiraoka Y (1990). Homeodomain of yeast repressor alpha 2 contains a nuclear localization signal. Proc Natl Acad Sci USA 87, 6954–6958.

Hall MN, Johnson AD (1987). Homeo domain of the yeast repressor alpha 2 is a sequence-specific DNA-binding domain but is not sufficient for repression. Science 237, 1007–1012.

Hammond-Martel I, Yu H, Affar el, B (2012). Roles of ubiquitin signaling in transcription regulation. Cell Signal 24, 410–421.

Han GS, Siniossoglou S, Carman GM (2007). The cellular functions of the yeast lipin homolog PAH1p are dependent on its phosphatidate phosphatase activity. J Biol Chem 282, 37026–37035.

Hickey CM (2016). Degradation elements coincide with cofactor binding sites in a short-lived transcription factor. Cell Logist 6, e1157664.

Hickey CM, Hochstrasser M (2015). STUbL-mediated degradation of the transcription factor MATalpha2 requires degradation elements that coincide with corepressor binding sites. Mol Biol Cell 26, 3401–3412.

Hirota K, Tsuda M, Murai J, Takagi T, Keka IS, Narita T, Fujita M, Sasanuma H, Kobayashi J, Takeda S (2014). SUMO-targeted ubiquitin ligase RNF4 plays a critical role in preventing chromosome loss. Genes Cells 19, 743–754.

Hochstrasser M, Ellison MJ, Chau V, Varshavsky A (1991). The short-lived MAT alpha 2 transcriptional regulator is ubiquitinated in vivo. Proc Natl Acad Sci USA 88, 4606–4610.

Hochstrasser M, Varshavsky A (1990). In vivo degradation of a transcriptional regulator: the yeast alpha 2 repressor. Cell 61, 697–708.

Huyer G, Piluek WF, Fansler Z, Kreft SG, Hochstrasser M, Brodsky JL, Michaelis S (2004). Distinct machinery is required in Saccharomyces cerevisiae for the endoplasmic reticulum-associated degradation of a multispanning membrane protein and a soluble luminal protein. J Biol Chem 279, 38369–38378.

Inobe T, Matouschek A (2014). Paradigms of protein degradation by the proteasome. Curr Opin Struct Biol 24, 156–164.

Johnson PR, Swanson R, Rakhilina L, Hochstrasser M (1998). Degradation signal masking by heterodimerization of MATalpha2 and MATa1 blocks their mutual destruction by the ubiquitin-proteasome pathway. Cell 94, 217–227.

Kaiser FJ, Moroy T, Chang GT, Horsthemke B, Ludecke HJ (2003). The RING finger protein RNF4, a co-regulator of transcription, interacts with the TRPS1 transcription factor. J Biol Chem 278, 38780–38785.

Karpova TS, Chen TY, Sprague BL, McNally JG (2004). Dynamic interactions of a transcription factor with DNA are accelerated by a chromatin remodeller. EMBO Rep 5, 1064–1070.

Ke A, Mathias JR, Vershon AK, Wolberger C (2002). Structural and thermodynamic characterization of the DNA binding properties of a triple alanine mutant of MATalpha2. Structure 10, 961–971.

Kumar M, Mommer MS, Sourjik V (2010). Mobility of cytoplasmic, membrane, and DNA-binding proteins in Escherichia coli. Biophys J 98, 552–559.

Laney JD, Hochstrasser M (2003). Ubiquitin-dependent degradation of the yeast Mat(alpha)2 repressor enables a switch in developmental state. Genes Dev 17, 2259–2270.

Longtine MS, McKenzie A 3rd, Demarini DJ, Shah NG, Wach A, Brachat A, Philippsen P, Pringle JR (1998). Additional modules for versatile and economical PCR-based gene deletion and modification in Saccharomyces cerevisiae. Yeast 14, 953–961.

Mead J, Zhong H, Acton TB, Vershon AK (1996). The yeast alpha2 and Mcm1 proteins interact through a region similar to a motif found in homeodomain proteins of higher eukaryotes. Mol Cell Biol 16, 2135–2143.

Mullen JR, Kaliraman V, Ibrahim SS, Brill SJ (2001). Requirement for three novel protein complexes in the absence of the Sgs1 DNA helicase in Saccharomyces cerevisiae. Genetics 157, 103–118.

Mumberg D, Muller R, Funk M (1995). Yeast vectors for the controlled expression of heterologous proteins in different genetic backgrounds. Gene 156, 119–122.

Nixon CE, Wilcox AJ, Laney JD (2010). Degradation of the Saccharomyces cerevisiae mating-type regulator alpha1: genetic dissection of cis-determinants and trans-acting pathways. Genetics 185, 497–511.

Oren M, Rotter V (2010). Mutant p53 gain-of-function in cancer. Cold Spring Harb Perspect Biol 2, a001107.

Rubenstein EM, Hochstrasser M (2010). Redundancy and variation in the ubiquitin-mediated proteolytic targeting of a transcription factor. Cell Cycle 9, 4282–4285.

Smith RL, Johnson AD (2000). A sequence resembling a peroxisomal targeting sequence directs the interaction between the tetratricopeptide repeats of Ssn6 and the homeodomain of alpha 2. Proc Natl Acad Sci USA 97, 3901–3906.

Sriramachandran AM, Dohmen RJ (2014). SUMO-targeted ubiquitin ligases. Biochim Biophys Acta 1843, 75–85.

Swanson R, Locher M, Hochstrasser M (2001). A conserved ubiquitin ligase of the nuclear envelope/endoplasmic reticulum that functions in both ER-associated and Matalpha2 repressor degradation. Genes Dev 15, 2660–2674.

Uzunova K, Gottsche K, Miteva M, Weisshaar SR, Glanemann C, Schnellhardt M, Niessen M, Scheel H, Hofmann K, Johnson ES, *et al.* (2007). Ubiquitin-dependent proteolytic control of SUMO conjugates. J Biol Chem 282, 34167–34175.

van de Pasch LA, Miles AJ, Nijenhuis W, Brabers NA, van Leenen D, Lijnzaad P, Brown MK, Ouellet J, Barral Y, Kops GJ, Holstege FC (2013). Centromere binding and a conserved role in chromosome stability for SUMO-dependent ubiquitin ligases. PLoS One 8, e65628.
Varshavsky A (2012). The ubiquitin system, an immense realm. Annu Rev Biochem 81, 167–176.
Vershon AK, Jin Y, Johnson AD (1995). A homeo domain protein lacking specific side chains of helix 3 can still bind DNA and direct transcriptional repression. Genes Dev 9, 182–192.
Vershon AK, Johnson AD (1993). A short, disordered protein region mediates interactions between the homeodomain of the yeast alpha 2 protein and the MCM1 protein. Cell 72, 105–112.
Wang X, Herr RA, Rabelink M, Hoeben RC, Wiertz EJ, Hansen TH (2009). Ube2j2 ubiquitinates hydroxylated amino acids on ER-associated degradation substrates. J Cell Biol 187, 655–668.
Wang Y (2014). RING finger protein 4 (RNF4) derepresses gene expression from DNA methylation. J Biol Chem 289, 33808–33813.
Weber A, Cohen I, Popp O, Dittmar G, Reiss Y, Sommer T, Ravid T, Jarosch E (2016). Sequential poly-ubiquitylation by specialized conjugating enzymes expands the versatility of a quality control ubiquitin ligase. Mol Cell 63, 827–839.
Wilcox AJ, Laney JD (2009). A ubiquitin-selective AAA-ATPase mediates transcriptional switching by remodelling a repressor-promoter DNA complex. Nat Cell Biol 11, 1481–1486.
Wolberger C, Vershon AK, Liu B, Johnson AD, Pabo CO (1991). Crystal structure of a MAT alpha 2 homeodomain-operator complex suggests a general model for homeodomain-DNA interactions. Cell 67, 517–528.
Xie Y, Kerscher O, Kroetz MB, McConchie HF, Sung P, Hochstrasser M (2007). The yeast Hex3.Slx8 heterodimer is a ubiquitin ligase stimulated by substrate sumoylation. J Biol Chem 282, 34176–34184.
Xie Y, Rubenstein EM, Matt T, Hochstrasser M (2010). SUMO-independent in vivo activity of a SUMO-targeted ubiquitin ligase toward a short-lived transcription factor. Genes Dev 24, 893–903.
Yang L, Mullen JR, Brill SJ (2006). Purification of the yeast Slx5-Slx8 protein complex and characterization of its DNA-binding activity. Nucleic Acids Res 34, 5541–5551.
Yin Y, Seifert A, Chua JS, Maure JF, Golebiowski F, Hay RT (2012). SUMO-targeted ubiquitin E3 ligase RNF4 is required for the response of human cells to DNA damage. Genes Dev 26, 1196–1208.
Zattas D, Hochstrasser M (2015). Ubiquitin-dependent protein degradation at the yeast endoplasmic reticulum and nuclear envelope. Crit Rev Biochem Mol Biol 50, 1–17.
Zhang C, Roberts TM, Yang J, Desai R, Brown GW (2006). Suppression of genomic instability by SLX5 and SLX8 in Saccharomyces cerevisiae. DNA Repair (Amst) 5, 336–346.
Zheng L, Baumann U, Reymond JL (2004). An efficient one-step site-directed and site-saturation mutagenesis protocol. Nucleic Acids Res 32, e115.